SECOND EUROPEAN CONFERENCE ON EARTHQUAKE ENGINEERING
AND SEISMOLOGY, ISTANBUL AUG. 25-29, 2014

EVALUATION OF APPROXIMATE METHODS TO ESTIMATE RESIDUAL DRIFT DEMANDS

Jorge RUIZ-GARCIA[1] and Carlos CHORA[2]

ABSTRACT

This paper presents the evaluation of two approximate methods recently proposed in the literature to estimate residual (permanent) drift demands at the end of earthquake excitation for seismic assessment of buildings. Both methods requires an estimate of the peak (maximum) interstory drift demand and the corresponding drift demand at significant yielding of the building. For this purpose, five moment-resisting steel framed buildings having different number of stories were analyzed under four sets of earthquake ground motions. Quantification of the accuracy of the approximate methods to estimate residual drift demands obtained from nonlinear time-history analyses was performed through the mean standard error computed for each building and each set of earthquake ground motions. Results show that the mean standard error tends to increase as the seismic hazard level increases. Between the two methods, the method introduced by Erochko et al. (2011) seems more effective in predicting residual drift demands than that proposed in FEMA P-58 (2012) recommendations in the US. It is demonstrated that including additional sources of stiffness and strength (e.g., slab participation in beams, interior gravity frames, and bending strength of shear-type connections in gravity frames) in the modeling approach constrain the amplitude of residual drift demands. As a benefit consequence, the accuracy of both approximate methods in predicting residual drift demands in significantly improved (i.e., mean standard error decreases).

INTRODUCTION

Recent seismic events have highlighted the necessity of demolishing damaged structures due to excessive permanent lateral deformations at the end of the earthquake ground shaking, even though they did not experience severe damage or collapse. For instance, after examining 12 low-to-mid-rise steel office buildings (particularly 10 with structural system based on steel moment-resisting frames) structurally damaged and leaned after the 1995 Hyogo-Ken-Nambu (Kobe) earthquake, Iwata et al. (2006) highlighted that the cost of repair leaned steel buildings linearly increased as the maximum and roof residual drift increased. Based on their study, the authors suggested that steel buildings should be limited to maximum and roof residual drift limits of about 1.4% and 0.9%, respectively, to satisfy a repairability limit state that meet both technical and economical constraints. More recently, a field investigation in Japan highlighted that a residual inter-story drift of about 0.5% is perceptible for building occupants and a residual inter-story drift of about 1.0% could cause human discomfort (McCormick et al., 2008). Therefore, several researchers have highlighted that the estimation of residual drift demands should also play an important role during the design of new buildings and,

[1] Professor, Universidad Michoacana de San Nicolás de Hidalgo, Morelia, jruizgar@stanfordalumni.org
[2] Graduate Research Assistant, Universidad Michoacana de San Nicolás de Hidalgo, Morelia.

particularly, the evaluation of the seismic structural performance of existing buildings (e.g., Pampanin et al., 2002; Ruiz-García and Miranda, 2006).

Prior studies have noted several important issues about the amplitude and height-wise distribution of residual drift demands in multi-degree-of-freedom systems (e.g., Pampanin et al., 2002; Ruiz-García et al., 2006). For instance: 1) the uncertainty (i.e., record-to-record variability) of residual drift demands is larger than that of peak (maximum) transient drift demands; 2) an increment in post-yield stiffness constrain the level of residual drift demands; 3) the structural overstrength diminishes the amplitude of residual drift demands; and 4) buildings having structural members with stiffness-and-strength degrading features (e.g., reinforced concrete buildings) experience smaller residual drift demands than those triggered in buildings that include structural members with non-degrading features (e.g., steel buildings). Among the aforementioned issues, the large record-to-record variability of residual drift demands found in analytical studies has made the estimation of this seismic parameter challenging during the performance-based assessment of existing buildings. With this aim, Erochko et al. (2011) and FEMA P-58 (2012) guidelines in the US have proposed simple expressions to estimate residual drift demands in buildings.

The objective of this paper is to present the results of a study aimed at the evaluation of two approximate methods proposed in the literature to estimate residual drift demands in buildings. For this purpose, five moment-resisting steel framed buildings having different number of stories were analyzed under four sets of earthquake ground motions. Quantification of the accuracy of the approximate methods to estimate residual drift demands obtained from nonlinear time-history analyses was performed through the mean standard error computed for each building and each set of earthquake ground motions.

REVIEW OF APPROXIMATE METHODS TO ESTIMATE RESIDUAL DRIFTS

Unlike methods to estimate peak inelastic displacement demands, very few methods have been proposed to estimate residual (permanent) displacement demands, particularly for multi-degree-of-freedom (MDOF) systems. In the author's knowledge, only the methods by Erochko et al. (2011) and FEMA P-58 (2012) have been introduced for this task.

Erochko-Christopoulos-Tremblay Method (2011)

Erochko et al. (2011) performed nonlinear dynamic analyses of a family of steel buildings having 2, 4, 6, 8, 10, and 12 stories. Two-dimensional (2D) models of the East-West and North-South directions, having steel moment-resisting frames and buckling-restrained braces as lateral load resisting systems, respectively, were analyzed under two sets of 20 earthquake ground motions (EQGMs). Both sets of EQGMs were originally developed as part of the SAC Joint Venture steel project (Somerville et al., 1997) and they represent two different seismic hazard levels (i.e., 10% probability of exceedance in 50 years and 2% probability of exceedance in 50 years).

Based on their analytical results, Erochko et al. (2011) proposed the following equation to estimate the expected residual drift, Δ_r, ratio of a given structure as follows:

$$\Delta_r = \left(\Delta_{\max} - \Delta_{el}\right) \times \frac{DCF}{2.5} \tag{1}$$

where $\Delta_{\max}$ is the maximum (peak) interstory drift, Δ_{el} is the recoverable elastic drift, and DCF is the drift concentration factor, which is defined as the ratio of the peak interstory drift divided by the maximum roof drift. According to Erochko et al. (2011), Δ_{el} is computed from the yield shear of the story with the largest residual drift divided by the elastic stiffness of that story.

FEMA P-58 Method (2012)

It is worth nothing that the up-to-date guidelines for the seismic performance assessment of buildings in the US (FEMA P-58, 2012) require an estimate of the expected residual drift ratio, Δ_r, at each level to determine whether the building is repairable or not. For this purpose, FEMA P-58 guidelines provided the following expressions:

$$\Delta_r = \begin{Bmatrix} 0 \\ 0.3(\Delta - \Delta_y) \\ \Delta - 3\Delta_y \end{Bmatrix} \quad \begin{matrix} \Delta \le \Delta_y \\ \Delta_y < \Delta \le 4\Delta_y \\ 4\Delta_y < \Delta \end{matrix} \tag{2}$$

where Δ is the peak transient interstory drift (equivalent to $\Delta_{\max}$ in Eq. 1) and Δ_y is the story drift at first significant yielding.

BUILDINGS AND GROUND MOTIONS CONSIDERED IN THIS STUDY

Five steel moment-resisting frame buildings having 3, 4, 6, 9, and 13 stories were analyzed as part of this study. Two-dimensional frame analytical models that represent each building were prepared using the computational platform *OpenSees* (2014). Two analytical models were prepared for the 3-, 4-, and 9-story buildings in this investigation. The first model (denoted with the **X**NmE label, where **X** is the number of stories) only includes the exterior moment-resisting frame, while a second model (denoted with the **X**NmEI label, where **X** is the number of stories) incorporates several additional sources of lateral stiffness and strength. In the **X**NmE models, the exterior two-way frame in the East-West direction was modeled as two-dimensional (2D) centerline model with an additional fictitious column, which is a common modeling strategy in the U.S. The fictitious column carries the vertical (gravity) loading from the rest of building (i.e., vertical loading carried by the interior gravity columns) and is attached to the exterior frame model through rigid frame elements to experience the same lateral deformation at each floor. However, the fictitious column does not provide the additional lateral stiffness from the interior gravity columns. Unlike building models **X**NmE, **X**NmEI building models include explicitly one interior gravity frame. Due to the limited information found in the literature, the 6- and 13-story buildings were only analyzed under the second modeling assumptions.

For both analytical building models, beams and columns were modeled as two-dimensional, prismatic beam elements composed of an elastic beam element with semi-rigid rotational springs at the ends that concentrates their inelastic behavior (i.e., moment-rotation hysteretic behavior) according to what has been discussed in Lignos and Krawinkler (2011a). Fig. 1 illustrates the modeling strategy of a *gravity* bay and a moment-resisting frame. The hysteretic behavior in the rotational springs accounts for structural cyclic degradation (i.e., strength and stiffness degradation) using the modified Ibarra-Krawinkler (MIK) model, which is described in detail in Lignos (2011) and implemented in *OpenSees* platform (2014). The parameters of the backbone curve in the MIK model for beams were obtained from those proposed in Lignos and Krawinkler (2011a) based on calibration using experimental results of the small-scale connections employed in the one-eighth scale specimen. In addition, panel zone flexibility was taken into account in each building model following the modeling technique proposed in (ATC, 2010). It should be noted that the slab contribution was not taken into account in the beam's stiffness and strength for the **X**NmE building models, which is consistent with the modeling assumptions followed by Lignos and Krawinkler (2011b). However, the contribution of the slab was explicitly included in building models **X**NmEI by using a larger beam's moment of inertia and asymmetric moment-rotation hysteretic relationship (i.e., with moment capacity in the positive bending direction 10% greater than that in the negative bending direction). In addition, the moment capacity in the shear-type connections included in the interior frames of the **X**NmEI models was included in their moment-rotation hysteretic behaviour as shown in Fig. 2.

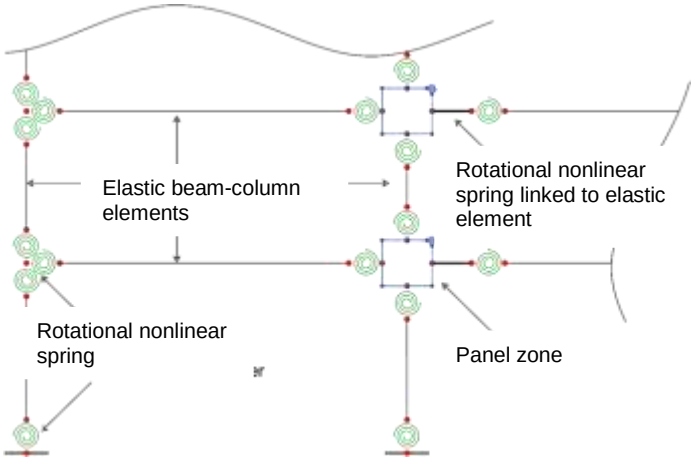

Figure 1. Nonlinear modeling strategy employed in the building models.

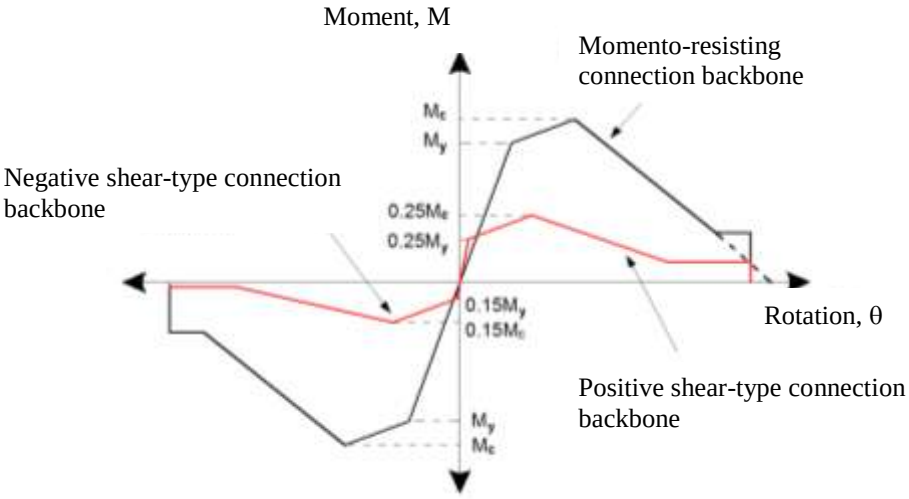

Figure 2. Moment-rotation hysteretic relationship employed for moment-resisting and shear-type connections.

In addition to identical modeling strategies in the exterior moment-resisting frame, building models **X**NmEI included two additional gravity-frame bays and one interior gravity frame. The interior beams were also modeled following the same modeling technique as the exterior beams, but their shear-type connections were modeled with the moment-rotation relationships shown in Fig. 2.

Before performing nonlinear dynamic analysis, conventional modal analysis and nonlinear static (*pushover*) analysis were carried out to obtain the dynamic and mechanical properties of both building models. For instance, Fig. 3 shows a comparison of the capacity curve corresponding to building models 4NmE and 4NmEI, while Table 1 reports relevant dynamic and mechanical features. From the figure, it can clearly be seen that the additional sources of stiffness and strength have significant influence in the capacity curve. For example, besides having larger initial stiffness (i.e., shorter period of vibration), the 4NmEI model has larger post-yield stiffness than the 4NmE model and the negative post-peak strength deterioration occurs at a larger roof drift. Therefore, it may be anticipated that the **X**NmEI building models would experience smaller residual drift demands as noted in previous studies (e.g. Ruiz-García and Miranda, 2006).

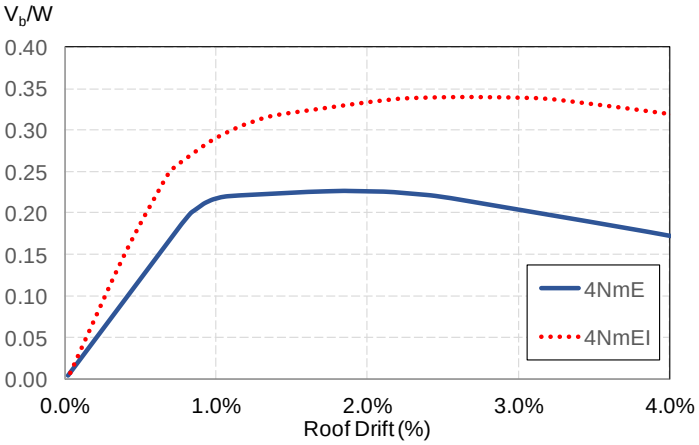

Figure 3. Comparison of capacity curves for the 4NmE and 4NmEI building models.

Table 1. Dynamic and mechanical properties of the building models

Building model	T_1 (s)	C_y	θ_y (%)	$\Gamma_1\Phi_1$
3NmE	1.04	0.34	1.10	1.29
3NmEI	0.92	0.38	0.80	1.28
4NmE	1.28	0.26	0.92	1.29
4NmEI	1.06	0.36	0.88	1.28
6NmE	1.4	0.20	0.60	1.29
9NmE	2.12	0.19	0.98	1.37
9NmEI	1.91	0.22	0.90	1.35
13NmE	3.04	0.13	0.80	1.35

Next, nonlinear dynamic time-history analyses were carried out using Newmark constant average acceleration method with time step equal to 0.001s to enhance convergence. Rayleigh damping equal to 3% of critical was assigned to the first and second modes. During the analysis, local P-delta effects were included (i.e., large displacement analysis).

The building models were subjected to four sets of earthquake ground motions. The first set contains 22 far-field earthquake ground motions recorded at firm sites assembled for the ATC-63 project to assess the collapse safety of modern reinforced concrete buildings. The remaining three sets of earthquake ground motions were assembled during the SAC project (Somerville et al., 1997) to evaluate the performance of typical steel office buildings in Los Angeles area prior to the 1994 Northridge earthquake, and they are representative of three seismic hazard levels at the site (e.g., 2% exceedance probability in 50 years).

EVALUATION PROCEDURE AND RESULTS

The approximate methods were evaluated using the following steps:
STEP 1: Estimation of the maximum (peak) transient drift ratio for the case-study building.
STEP 2: Estimation of the residual drift ratio using approximate methods.
2A. For the Erochko et al. (2011) method the residual drift ratio is estimated with the following steps:

Step a. Compute Δ_{el} as defined in Eq. 1.
Step b. Estimate the DCF as defined in Eq. 1 from the results of NLTH analysis.
Step c. Calculate the residual drift ratio, for the roof or a selected story, using Eq. 1

2B. For the FEMA P-58 method (2012) the residual drift ratio is estimated for a given earthquake ground motion with the following steps:

Step a. Compute Δ_y from nonlinear static pushover analysis. Δ_y can corresponds to the roof or a selected story (e.g., the first story).
Step b. Check which interval in Eq. 2 corresponds to the computed peak drift ratio.

Step c. Calculate the residual drift ratio, for the roof or a selected story, using Eq. 2.

STEP 3: Compute ratios of approximate to exact residual drift ratios. These ratios were computed for all combinations of earthquake ground motions and period of vibration.

STEP 4: Compute central tendency and dispersion measures.

STEP 5: Compute a global error measure. In this investigation, both the logarithmic standard error, $\varepsilon_{\ln}$, and the mean standard error, ε, were used as error measures and they are defined as follows:

$$\varepsilon = \sqrt{\frac{1}{n}\sum_{i=1}^{n}\left(\Delta_{r,NLTH,i} - \Delta_{r,a,i}\right)^2} \tag{3}$$

$$\varepsilon_{\ln} = \sqrt{\frac{1}{n}\sum_{i=1}^{n}\left(\ln\left(\frac{\Delta_{r,NLTH,i}}{\Delta_{r,a,i}}\right)\right)^2} \tag{4}$$

where n is the number of earthquake ground motions included in each set, $\Delta_{r,a,i}$ is the residual drift ratio computed from the approximate method corresponding to the i-th earthquake ground motion and $\Delta_{r,NLTH,i}$ is the residual drift ratio computed from nonlinear time-history (NLTH) analysis corresponding to the same earthquake ground motion.

Fig. 4 shows the median residual interstory drift ratio (RIDR) demand profiles corresponding to each of the building models including exterior frames when subjected to each of the four earthquake ground motion sets. RIDR profiles are shown with respect to normalized height z/H, where z is the relative height with respect to the ground and H is the total height, for the sake of comparison of trends. It can clearly be seen that the FF and LA 50/50 trigger negligible RIDR demands for all building models. The set LA 10/50 triggers residual drift demands that might cause human perception in building models 3NmE and 4NmE, while the set LA 2/50 lead to significant increment in RIDR demands. Particularly, building models 3NmE, 4NmE and 13NmE experiences RIDR demands close to, or in excess of, 2% under this set, which may cause their demolition.

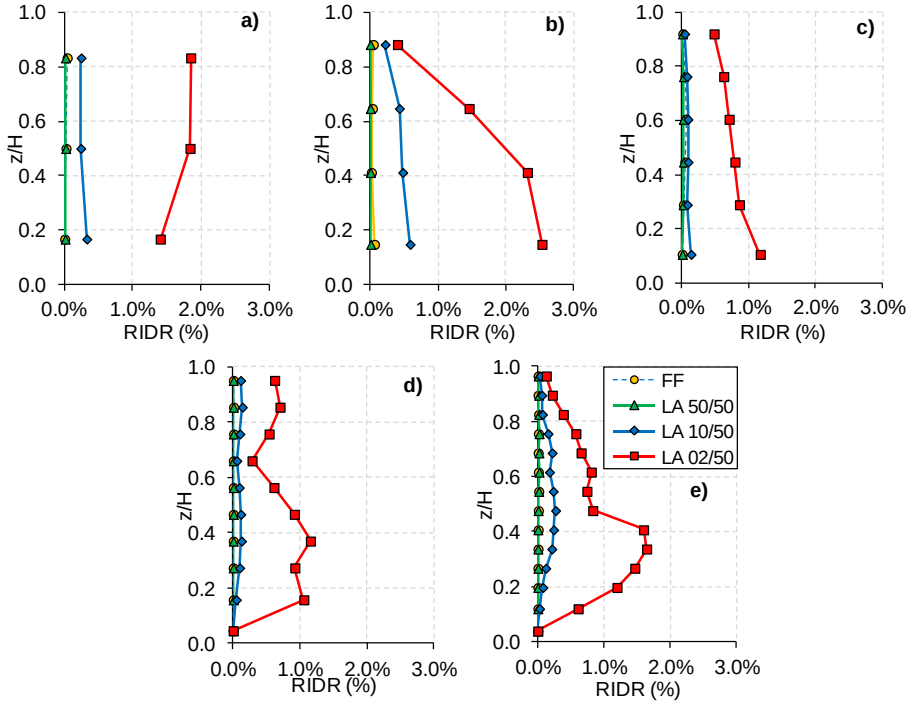

Figure 4. Median residual interstory drift ratio (RIDR) profiles obtained for each building model including exterior frames: a) 3NmE; b) 4NmE; c) 6NmE; d) 9NmE; and 13NmE.

Fig. 5 illustrates the height-wise distribution of median RIDR demands for the building models including both exterior and interior frames when subjected to each of the four earthquake ground motion sets. Comparing Figs. 4 and 5 allows examining the influence of the modelling approach (i.e., including additional sources of stiffness and strength in the building models) on the amplitude of RIDR demands for the 3-story, 4-story, and 9-story building. It can be observed that latter models experiences smaller RIDR demands, particularly under the LA 10/50 and LA 2/50 sets. This observation is in good agreement from previous findings of Ruiz-Garcia and Miranda (2006), which noted that structural overstrength in one-bay generic frame models diminishes the amplitude of residual drift demands. Therefore, it should be highlighted that neglecting additional sources of stiffness and strength overestimate the amplitude of residual drift demands.

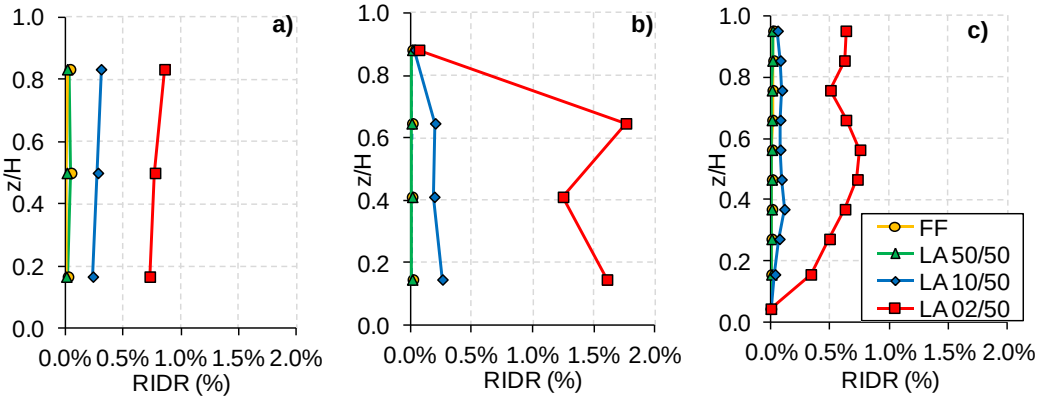

Figure 5. Median residual interstory drift ratio (RIDR) profiles obtained for each building model including exterior and interior frames: a) 3NmE; b) 4NmE; and c) 9NmE.

In this study, both the ε and $\varepsilon_{\ln}$ for predicting residual drift demands using each approxiamte method were computed for each building model (including or not including additional sources of stiffness and strength) when subjected to each set of earthquake ground motions. Error plots were prepared for building models modelled with only exterior frame (**X**NmE label, where **X** is the number of stories) and with exterior and interior frames (**X**NmEI label, where **X** is the number of stories) as described in the above section. For instance, Fig. 6 shows a comparison of ε of the first-story residual drift demand for the building models with only exterior frame, while Fig. 7 shows a similar comparison for the building models with both exterior and interior frames.

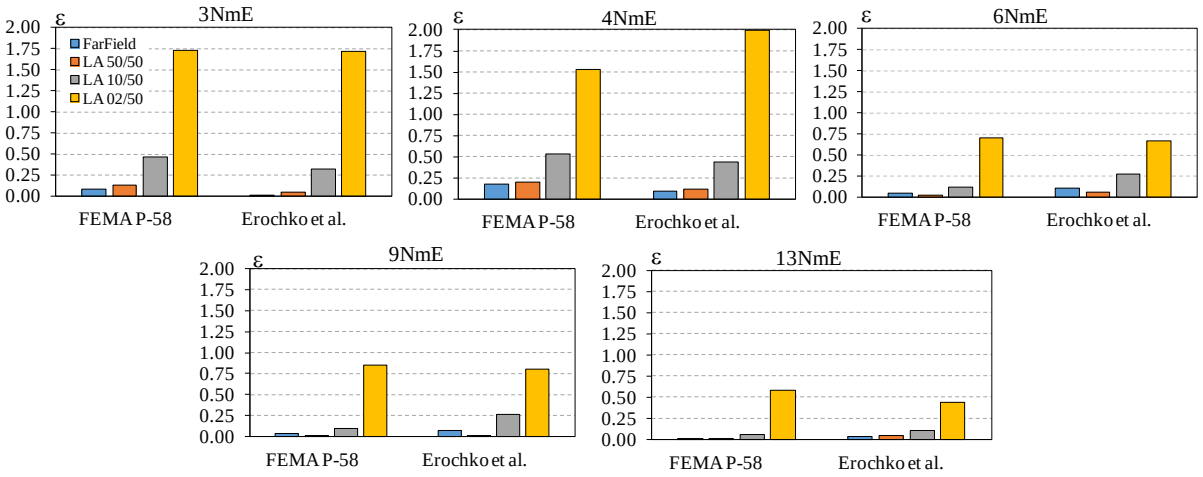

Figure 6. Mean standard error computed for each approximate method and each earthquake ground motion set corresponding to building models with exterior frame.

From both figures, it can clearly be seen that the lowest errors for both approximate methods are obtained from the FF and the LA 50/50 earthquake ground motion sets regardless of the building modelling. For this earthquake ground motion sets, the method proposed by Erochko et al. (2011) lead to smaller errors than that suggested in FEMA P-58 (2012). In general, two tendencies can be observed from the figures: 1) ε increases as the seismic hazard increases, 2) ε tends to decrease as the period of vibration (i.e., number of stories) increases. It can also be observed that the modelling approach has significant impact in ε since standard errors computed from building models that include both exterior and interior frames are smaller that those computed form building models that only include the exterior frame.

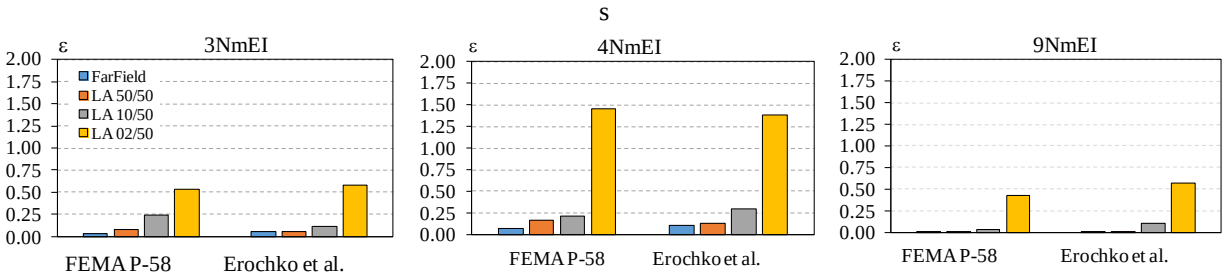

Figure 7. Mean standard error computed for each approximate method and each earthquake ground motion set corresponding to building models with exterior and interior frames.

Next, Fig. 8 illustrates a comparison of $\varepsilon_{\ln}$ of the first-story residual drift demand for the building models with only exterior frame, while Fig. 9 shows a similar comparison for the building models with both exterior and interior frames. Unlike the mean standard error, in general, the mean logarithmic error does not show a clear general trend and the error should be judged in a case-by-case manner. For instance, comparing the $\varepsilon_{\ln}$ for building models 3NmE and 3NmEI, it seems that adding sources of stifness and overstrength in the building model leads a better prediction of the approximates methods (i.e., $\varepsilon_{\ln}$ decreases). However, this is not the case of building models 4NmE and 4NmEI.

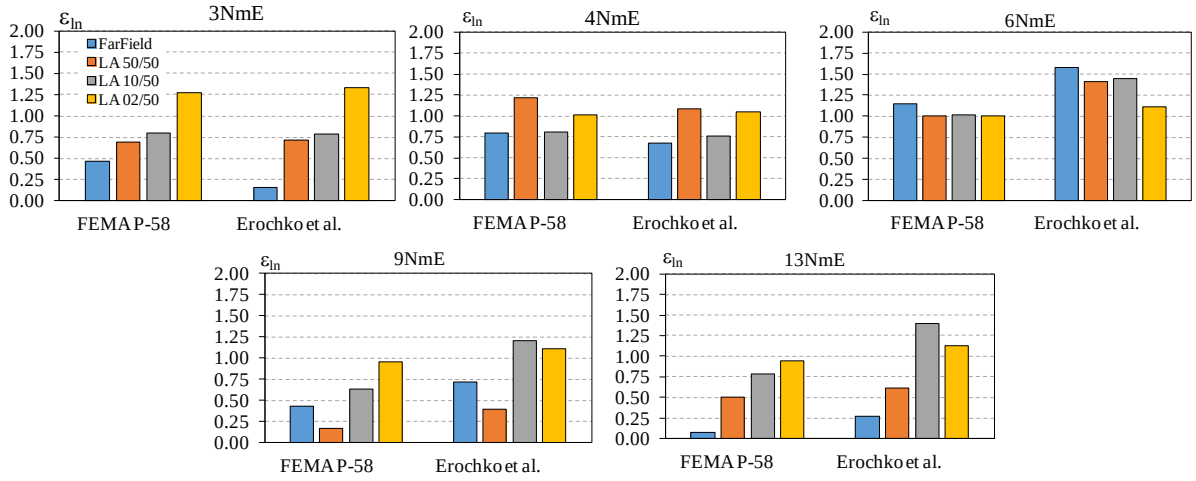

Figure 8. Mean logarithmic error computed for each approximate method and each earthquake ground motion set corresponding to building models with exterior frame.

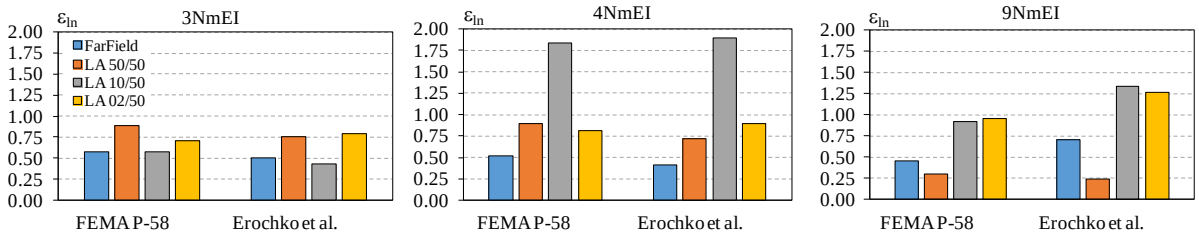

Figure 9. Mean logarithmic error computed for each approximate method and each earthquake ground motion set corresponding to building models with exterior and interior frames.

It is instructive to examine in more detail the evolution of standard error. For instance, Fig. 10 shows the scatter diagram of the approximate, $\Delta_{r,approx}$, and calculated, $\Delta_{r,NLTH}$, residual displacements for the 4-story building modeled with only exterior frame (upper row) and both exterior-interior frames (lower row) when subjected to three sets of earthquake ground motions with different hazard level. The standard error computed for both approximate methods is also included in the figure. It can clearly be seen that ε computed for both methods increases as the seismic hazard increases. Although both methods provide a resonable prediction of first-story residual drift demands under the LA 50/50 and LA 10/50 sets, very large ε results when the both building models are subjected to the LA 2/50 set. It should be noted that both building models experience very low levels of residual drift, or even remains in the same position at the end of the earthquake excitation, under most of the earthquake ground motions included in set LA 50/50. This trend is captured by both methods leading to small ε. The incorporation of additional sources of siffness and strength in the building modelling has the beneficial effect of constraing residual drifts, which can be explained since the **X**NmEI models exhibit larger post-yield stiffness than the **X**NmE models. As a consequence, smaller standard errors were computed in the former models than those in the latter building models (e.g., comparing plots in the upper and lower row in Fig. 10).

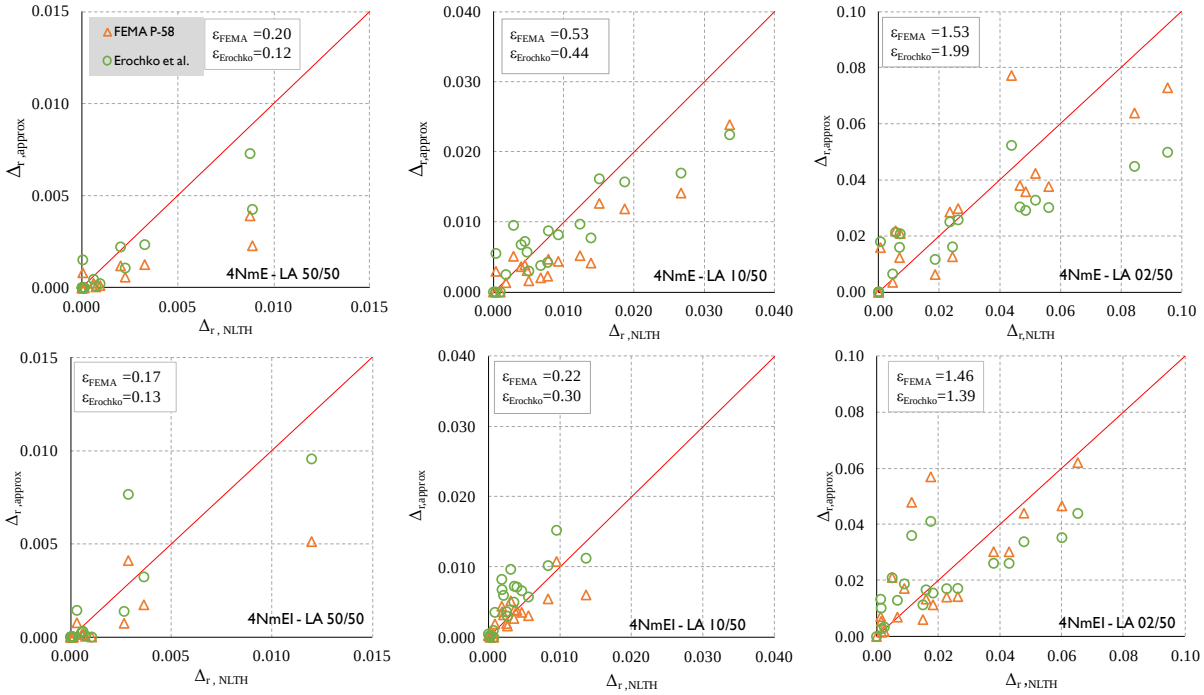

Figure 10. Scatter diagrams of approximate and calculated residual displacements for the 4-story building models.

CONCLUSIONS

Two approximate methods to estimate residual drifts demands in buildings were evaluated as part of this ongoing investigation. Both methods require an estimation of the peak (maximum) transient and the interstory drift at first significant yielding. The approximate methods were used to obtain estimates of residual drift demands in five steel buildings having different number of stories (i.e., fundamental period of vibration). The five case-study buildings were modelled through a 2D exterior steel moment-resisting frame, which is the traditional modelling approach in the US. In addition, three of them were also modelled as 2D parallel frames that include one exterior frame (moment-resisting frame) and one interior frame (that represents the interior gravity frames in a consolidated way). From pushover analysis, it was shown that the latter building models have larger strength as well as initial and post-yield stiffness that their corresponding traditional building models. Residual drift demands were computed through nonlinear time history (NLTH) analyses for all 8 building models when subjected to 4 different sets of earthquake ground motions. To quantify the accuracy of each approximate method to estimate residual drift demands, the mean standard error, ε , and the mean logarithmic error, $\varepsilon_{\ln}$, were computed for each building and each earthquake ground motion set.

Results of this investigation clearly showed that the modelling approach has significant impact in the amplitude of residual drift demands. Particularly, including additional sources of stiffness and strength led to larger post-yield stiffness that constrained the amplitude of residual drift demands. Using ε , it was noted that the accuracy of both approximate methods to predict residual drift demands decreases as the intensity of the earthquake ground motions increases (i.e., with higher hazard level). Comparing both approximate methods, it seems that the method proposed by Erochko et al. (2011) provides better prediction of residual drift demands than that proposed in FEMA P-58 (2012).

ACKNOWLEDGEMENTS

The authors express their gratitude to the *Consejo Nacional de Ciencia y Tecnología* (CONACYT) in Mexico for funding the research reported in this paper. They also would like to thank the *Universidad Michoacana de San Nicolás de Hidalgo.*

REFERENCES

Applied Technology Council (ATC) (2010) Modeling and acceptance criteria for seismic design and analysis of tall buildings, ATC 72-1, Redwood City, CA, USA.

Erochko J, Christopoulos C, Tremblay R, Choi H (2011) "Residual drift response of SMRFs and BRB frames in steel buildings designed according to ASCE 7-05", *J. of Struct. Eng.*, 137(5):589–599

FEMA P-58 (2012) Seismic performance assessment of buildings, Vol. 1-2. Washington, D.C.

Iwata Y, Sugimoto H, Kuguamura H (2006) "Reparability limit of steel structural buildings based on the actual data of the Hyogoken-Nanbu earthquake", *Proceedings of the 38th Joint Panel. Wind and Seismic effects*. NIST Special Publication 1057, 23-32

Lignos D (2008) "Sidesway collapse of deteriorating structural systems under seismic excitations", PhD. Thesis, Stanford University, CA.

Lignos D, Krawinkler H (2011a) "Deterioration modeling of steel components in support of collapse prediction of steel moment frames under earthquake loading", *J. of Struct. Eng.*, 137(11):1291–1302

Lignos D, Krawinkler H (2011b) "Prediction and validation of sidesway collapse of two scale models of a 4-story steel moment frame", *Earthquake Engineering and Structural Dynamics*; 40:807–825.

McCormick J, Aburano H, Ikenaga M, Nakashima, M (2008) "Permissible residual deformation levels for building structures considering both safety and human elements", *Proceedings of the 14th World Conference on Earthquake Engineering*, Beijing, China, Paper No. 05-06-0071

OpenSees. (2014). "Open System for Earthquake Engineering Simulation - Home Page." <http://opensees.berkeley.edu/> (April 1, 2014).

Pampanin S, Christopoulos C, Priestley MJN (2003) "Performance-based seismic response of framed structures including residual deformations. Part II: Multiple-degree-of-freedom systems", *Journal of Earthquake Engineering*, 7 (1): 119-147

Ruiz-García J, Miranda E (2006) "Evaluation of residual drift demands in regular multi-story frame buildings for performance-based assessment", *Earthquake Engineering and Structural Dynamics*, 35 (13): 1609-1629

Somerville PG, Smith N, Punyamurthula S, and Sun J (1997) "Development of ground motion time histories for phase 2 of the FEMA/SAC Steel Project", Report SAC/BD-97/04, SAC Joint Venture.

Zareian F, Medina RA (2009) "A practical method for proper modeling of structural damping in inelastic plane structural systems", *Computers & Struct*, 88:45-53